

High temperature dispersion strengthening of NiAl

MARK SHERMAN

Sohio Research Center, Cleveland, Ohio, USA

KRISHNA VEDULA

Department of Metallurgy and Materials Science, Case Western Reserve University, Cleveland, Ohio, USA

A potential high temperature strengthening mechanism for alloys based on the intermetallic compound NiAl has been investigated. This study forms part of an overall program at NASA Lewis Research Center for exploring the potential of alloys based on NiAl for high temperature applications. An alloy containing 2.26 at% Nb and produced by hot extrusion of blended powders has been examined in detail using optical and electron microscopy. Interdiffusion between the blended niobium and NiAl powders results in the formation of intermediate phases. A fine dispersion of precipitates of a hexagonal, ordered NiAlNb phase in a matrix of NiAl can be produced and this results in strengthening of the alloy by interfering with dislocation motion at high temperature. These precipitates are, however, found to coarsen during the high temperature (1300 K) deformation at slow strain rates and this may impose some limitations on the use of this strengthening mechanism.

1. Introduction

Ordered intermetallics have long been recognized as candidates for high temperature applications because thermally activated processes such as diffusion are inhibited by the ordered crystal structure. Recently, interest has been generated in developing certain intermetallic compounds for high temperature applications [1–4]. The ordered intermetallic NiAl is especially attractive since this compound offers oxidation and corrosion resistance, remains ordered up to its high congruent melting point of 1913 K, and has a density advantage over conventional superalloys because of its high aluminium content.

The drawbacks of NiAl, however, are its room temperature brittleness and its inadequate creep resistance at high temperatures, in spite of its ordered crystal structure. In this paper, we are concerned only with its high temperature mechanical properties. Previous work [5] has shown that the high temperature creep resistance of NiAl can be improved to levels comparable with those of some superalloys by macroalloying with ternary additions, using a powder metallurgy process. The powder metallurgy process involves blending of elemental ternary additions with binary NiAl followed by hot extrusion in a sealed steel container. Additions of niobium, tantalum and hafnium at the 2 at% level, in particular, have shown the most promise. The reasons for this improvement in high temperature creep resistance are, nevertheless, not clear.

The purpose of this study was to understand the interaction between the niobium powder and the NiAl powder during the powder metallurgy processing of an alloy containing 2.26 at% Nb and to identify the

mechanism of high temperature strengthening in this alloy. This alloy has been microscopically examined before and after high temperature deformation in order to obtain this understanding.

2. Materials and procedure

The alloy was prepared at NASA Lewis Research Center by blending approximately 2 at% of –325 mesh commercially pure niobium powder, with –80 mesh prealloyed NiAl powder. The fine niobium powder was used in order to enhance interdiffusion between the matrix NiAl and the ternary addition. The powder blend was filled in a mild steel can (5 cm diameter and 12.5 cm long) which was evacuated and sealed. The sealed can was preheated to a temperature of 1366 K and extruded through a vertical die at an area reduction ratio of 16:1. The extruded can was air cooled and the steel can was then removed by grinding. The alloy specimens were subsequently homogenized at 1523 K in argon for 175 h to ensure maximum interdiffusion between the ternary addition and the matrix NiAl. Spectrographic analysis of the as-homogenized alloy showed the alloy to have a nominal chemical composition of 50.19 at% Ni, 47.58 at% Al and 2.26 at% Nb.

Cross-sections of the as-extruded and as-homogenized specimens were examined using optical and scanning electron microscopy. Cylindrical specimens (5 mm diameter and 10 mm long) of the as-homogenized material were prepared by centreless grinding. Specimens were tested (at NASA Lewis Research Center) in compression on an Instron Testing machine at a temperature of 1300 K, or $0.68T_m$, where T_m is the absolute melting temperature, and at

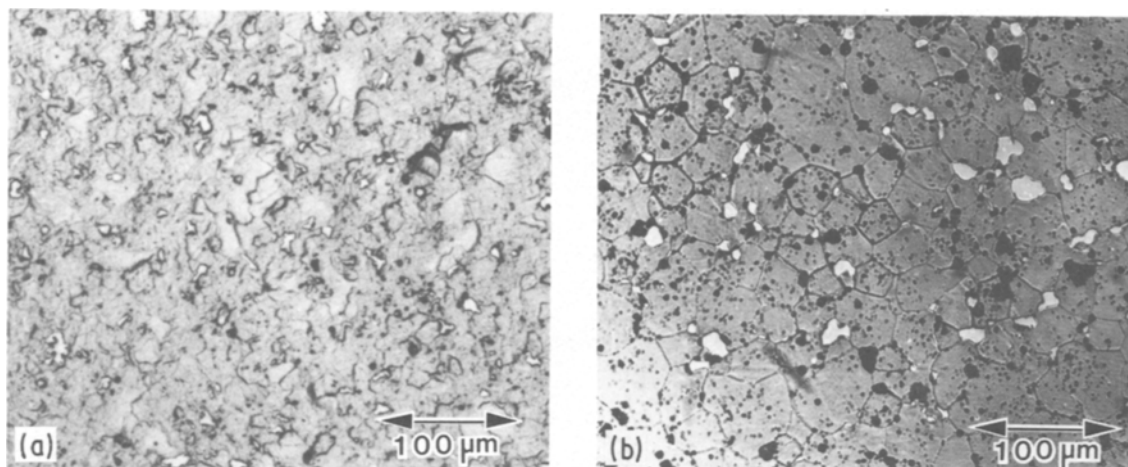


Figure 1 Comparison of optical micrographs of cross-sections of (a) as-extruded and (b) as-homogenized specimens of the NiAl-2.26 at % Nb alloy (Marbles Reagent Etch).

slow strain rates. The specimen tested at an initial strain rate of $3 \times 10^{-7} \text{ sec}^{-1}$ to a final strain of about 7% was examined in considerable detail using optical and scanning electron microscopy.

Transmission electron microscopy (TEM) of the specimens before and after compression testing was used to identify the second phases and to examine the substructure of the specimens in order to understand the strengthening mechanism. Thin foils for TEM were prepared by electropolishing in a 2:1 methanol/nitric acid solution cooled to 253 K.

3. Results and discussion

3.1. As-extruded and as-homogenized specimens

The as-extruded microstructure (illustrated in Fig. 1a) contains recrystallized NiAl grains with very little porosity. The second phase particles observed are the undissolved niobium particles which have a wide range of sizes, the average size being roughly $4 \mu\text{m}$.

The as-homogenized microstructure (illustrated in Fig. 1b) shows a well developed grain structure with an average grain size of about $25 \mu\text{m}$ which is somewhat larger than the as-extruded grain size. A slight increase in the amount of porosity is observed and is suspected to be due to pull out of particles during

specimen preparation. The average size of the second phase particles has increased by about 50% to roughly $5.5 \mu\text{m}$. The increase in size of the second phase particles, which were originally niobium powder particles, is believed to be a result of transformation of the niobium to a ternary intermetallic of nickel, aluminium and niobium by interdiffusion.

The distribution of the second phase particles is clearly observed in the scanning electron micrograph in Fig. 2a. Some of the larger particles reveal the presence of two phases, one surrounding the other, as illustrated in Fig. 2b. Energy dispersive analysis of X-rays from the two regions shows that the inner phase contains more niobium than the outer phase and the compositions of the phases correspond in general to the phases NiAlNb_2 and NiAlNb respectively (Fig. 3). A more definite confirmation of their compositions could not be made since standards were not used for the analyses. These two phases are in agreement with an earlier study by Kornilov *et al.* [6] on the phase equilibrium between NiAl and niobium. This kind of a layered structure results from incomplete interdiffusion between the matrix of NiAl and the elemental addition of niobium.

The pseudo-binary phase diagram for NiAl-Nb is reproduced in Fig. 4 from Kornilov *et al.* [6]. With

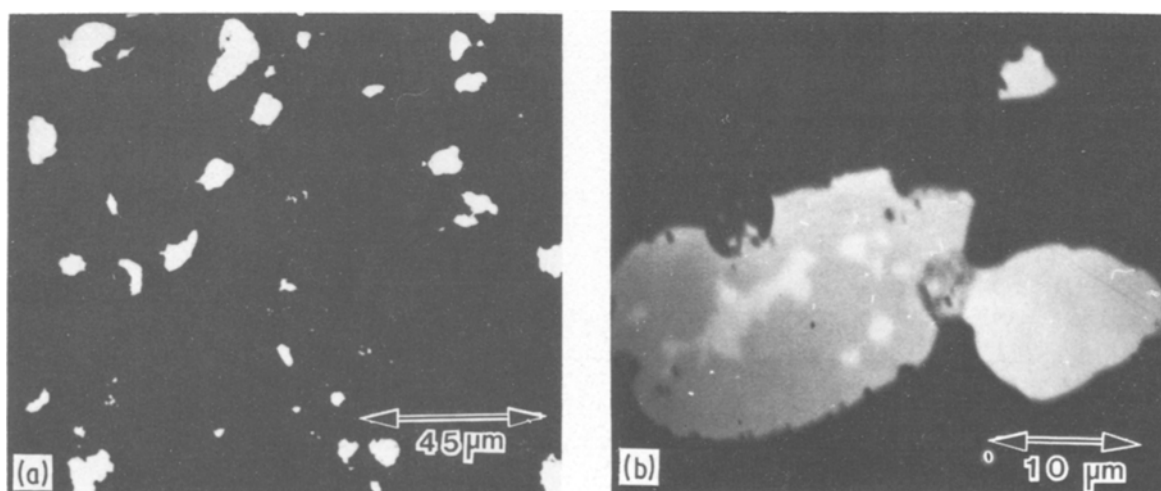


Figure 2 SEM backscattered electron images of the homogenized alloy showing (a) a typical distribution of niobium-rich particles and (b) the existence of a layered two-phase structure within some of the larger particles (cross-section).

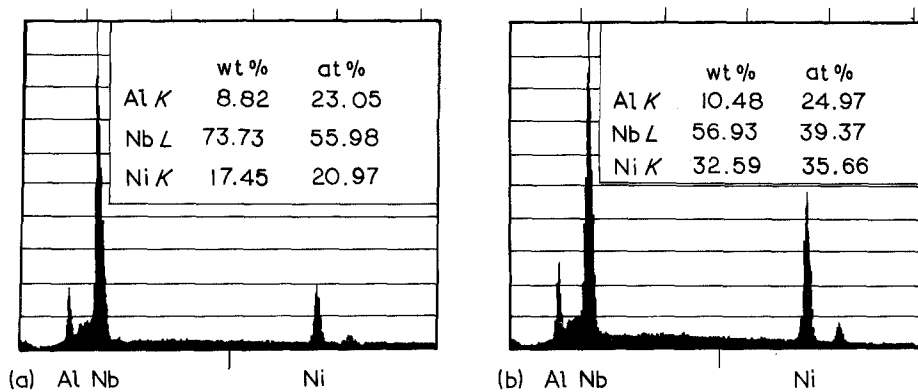


Figure 3 EDS analysis of the two regions of particle in Fig. 2b. (a) The inner phase corresponding roughly to NiAlNb₂ and (b) the outer phase corresponding roughly to NiAlNb.

increasing niobium, the phases present in this pseudo-binary section are NiAl (with a very limited solubility of niobium), NiAlNb and NiAlNb₂. NiAl and NiAlNb exhibit a eutectic at about 1710 K. The solubility of niobium in NiAl, according to this diagram is less than 1 at % at low temperatures, but increases significantly above about 1450 K and can approach 5 at % near the eutectic temperature. Hence, during the homogenization treatment (1523 K), the matrix of NiAl and the niobium powder particles act as a finite spherical diffusion couple and the phases corresponding to the two intermediate ternary intermetallics form between the NiAl and the niobium.

Since the solubility of niobium is much higher at the homogenization temperature than at room temperature, the slow cooling after the homogenization treatment results in reprecipitation of a second phase of NiAlNb in the matrix of NiAl. A distribution of very fine precipitates is, in fact, observed when a thin foil is examined on the Transmission Electron Microscope at a high magnification (Fig. 5a). These precipitates are, however, only 10 to 50 nm in size and too small to be detected at the low magnifications used in the

optical and scanning electron micrographs. A diffraction pattern showing the spots for the matrix as well as the precipitates is shown in Fig. 5b. The diffraction spot used to obtain the dark field image of the precipitates in Fig. 5a is indicated by the arrow in Fig. 5b.

3.2. Deformed specimen

Cylindrical specimens were tested at slow strain rates in compression and the behaviour of a specimen with an initial strain rate of $3 \times 10^{-7} \text{ sec}^{-1}$ is plotted in the form of a true stress-true plastic strain curve in Fig. 6 and compared with similar curves for binary NiAl [7]. Plastic flow in the ternary alloy is initiated at a stress of about 35.0 MPa which is significantly higher than that for the binary alloy, indicating a substantial strengthening due to the ternary addition. The flow stress, however, drops during the deformation to a lower value of about 29 MPa after a plastic strain of about 4%. A possible explanation for the strengthening can be obtained from an understanding of the microstructure of the tested specimen.

The matrix NiAl grains appear to have grown somewhat during the testing as evidenced by comparing

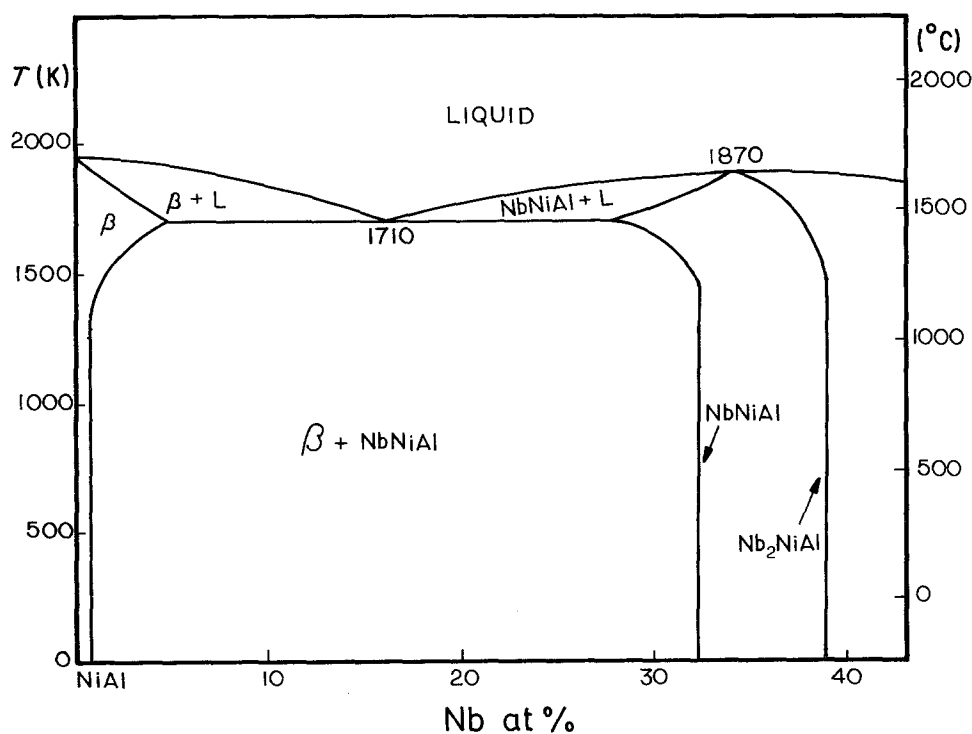


Figure 4 Pseudo-binary phase diagram of the NiAl-Nb system (Kornilov, [6]), L; liquid.

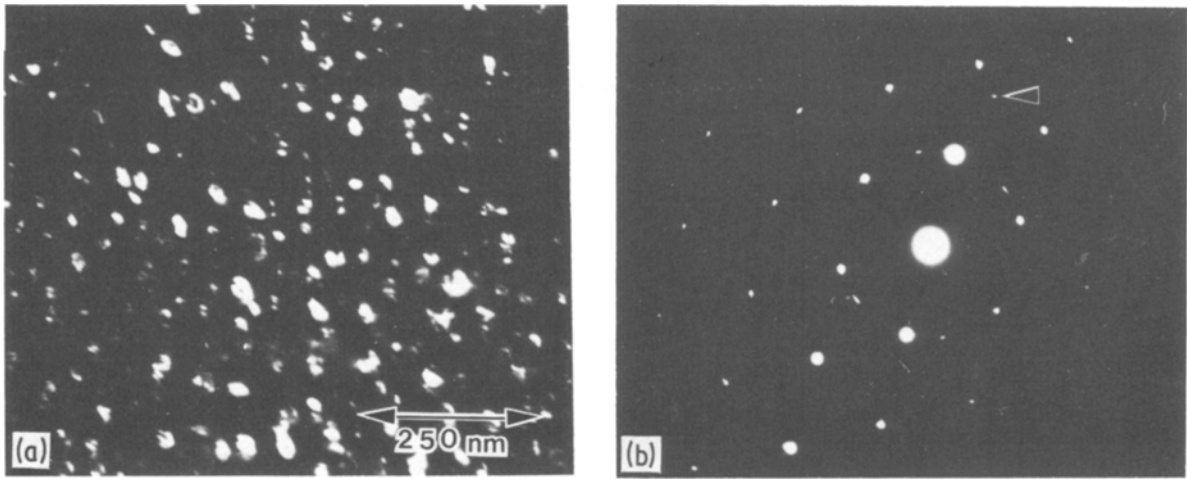


Figure 5 (a) TEM dark field image of precipitates in the homogenized alloy and (b) the corresponding diffraction pattern with arrow indicating the reflection used for imaging.

the optical microstructure of the tested specimen in Fig. 7a with that of the untested specimen in Fig. 1b. The average grain size measured shows an increase from about 25 to about 33 μm . A considerable amount of etch pitting within the grains is suspected to be associated with dislocations within these grains. Voids appear to have coalesced along the triple points and grain boundaries during the testing, presumably due to grain boundary sliding.

A striking feature of the deformed specimen when compared with the undeformed specimen is the presence of many precipitates within the grains of the deformed specimen when compared on the scanning electron microscope in the backscatter mode (Fig. 7b

compared with Fig. 2a). These precipitates are between 0.5 and 1 μm in size and much smaller than the original niobium powder particles. These precipitates have been shown to be NiAlNb precipitates and could be a result of coarsening of much finer precipitates which were not resolved on the SEM in the homogenized specimen.

An interesting aspect of the microstructure of the deformed specimen is the presence of regions around the large particles which are devoid of the fine precipitates. Such a precipitate-free zone must be a consequence of dissolution of smaller precipitates in the vicinity of the larger particles and redeposition on the surface of the larger particles due to Ostwald ripening.

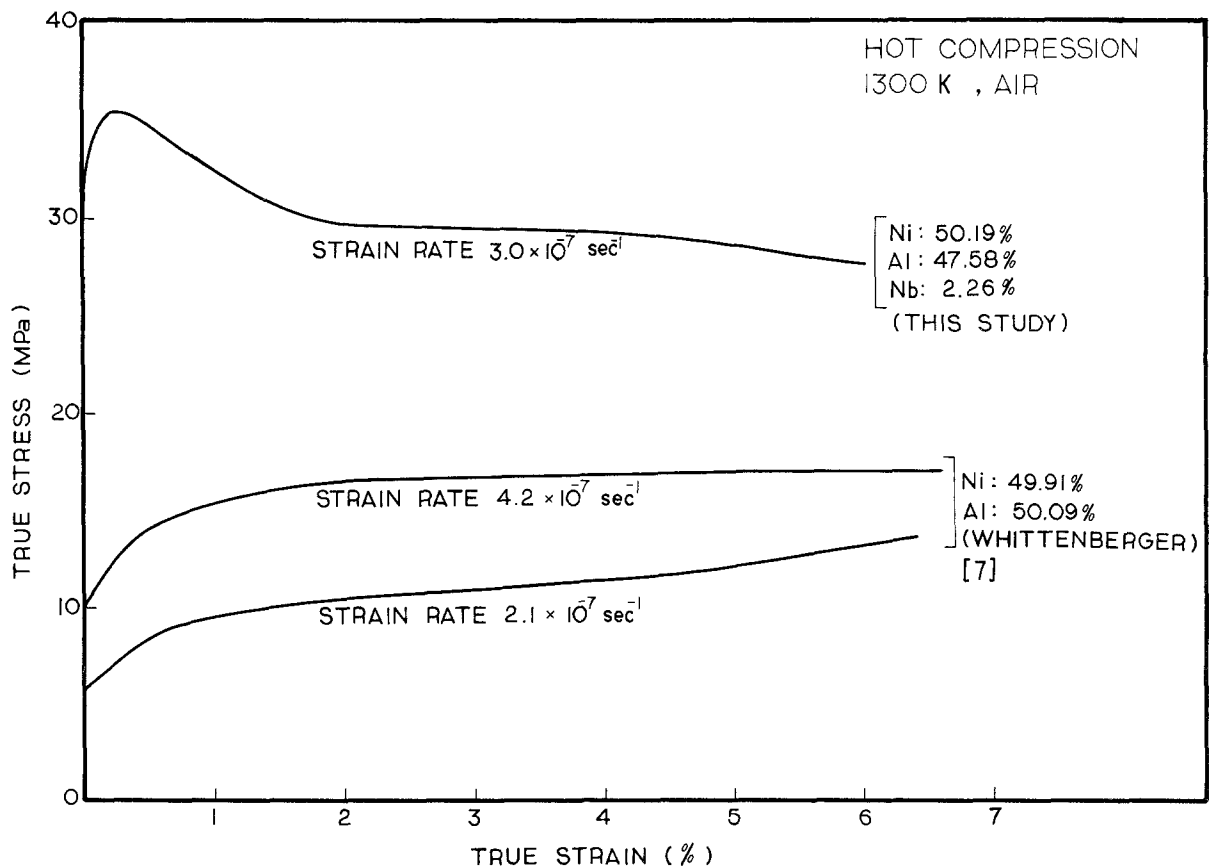


Figure 6 Comparison of the true stress-true plastic strain behaviour of the niobium containing alloy with a binary NiAl alloy [7]. Specimens tested in compression at 1300 K and slow strain rates.

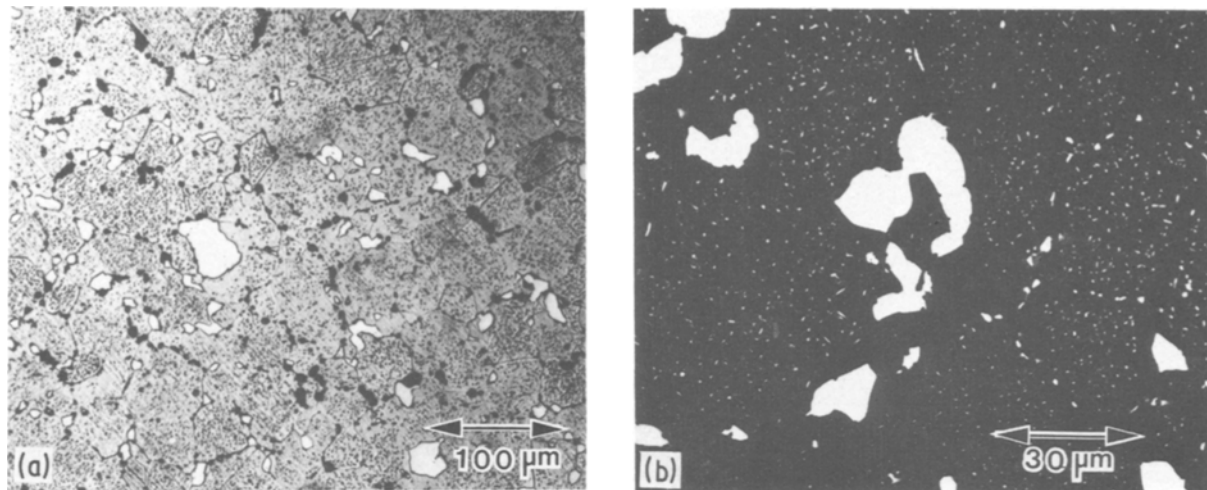


Figure 7 (a) Optical microstructure of specimen after testing showing grain boundary void formation (etched), (b) SEM backscattered electron image of same specimen showing coarsened NiAlNb precipitates and precipitate depleted regions around original niobium-rich particles.

Transmission electron microscopy of the deformed specimen reveals precipitates of the size of about 500 nm (Fig. 8), thus providing direct evidence that the precipitates have coarsened significantly during the high temperature testing (compare Fig. 5 with Fig. 8). The size of the precipitates observed in the transmission electron micrograph is in agreement with the size observed in the scanning electron micrograph of the tested specimen. A possible reason for the rapid coarsening during deformation may be increased diffusion through dislocation pipes.

3.3. Strengthening mechanism

The mechanism of strengthening in the ternary alloy is believed to be due to the interaction between the fine precipitates and dislocations. Dislocation bowing as well as development of dislocation networks between the precipitates are observed throughout the thin foil of the deformed specimen. Typical examples are illustrated in Figs 9a and b. This kind of interaction is generally observed when the precipitates act as obstacles to dislocation motion and hence strengthen the material [8–10].

Dislocation networks with segments parallel to $\langle 101 \rangle$ and $\langle 110 \rangle$ g vectors developed between precipi-

pitae particles. Curved dislocation lines are dominant at and near precipitates, whereas straight parallel dislocations were observed in groups in the matrix and piled up at elongated particles. Subgrain boundaries were observed at grain boundaries and at the precipitates. The Burgers vectors of dislocations in the deformed specimen were not uniquely determined. However, in general, the dislocations were strongly visible with (110) reflections and invisible with (112) reflections.

The identification of the precipitates which are believed to cause the strengthening was carried out using selected area and microdiffraction on the transmission electron microscope using the deformed specimen. The precipitates in the undeformed specimen were too small to be properly analysed and it is assumed that they have the same composition and crystal structure as those identified in the tested specimen. The precipitates in the deformed specimen are found to be NiAlNb with a hexagonal crystal structure. A TEM bright field image of one of the precipitates and the corresponding small angle diffraction (SAD) and microdiffraction patterns of a zone axis are shown in Fig. 10. Measurements from several diffraction patterns confirm the hexagonal phase NiAlNb. The d -spacings from the Inorganic Powder Diffraction File for NiAlNb and those measured from electron diffraction patterns are presented in Table I.

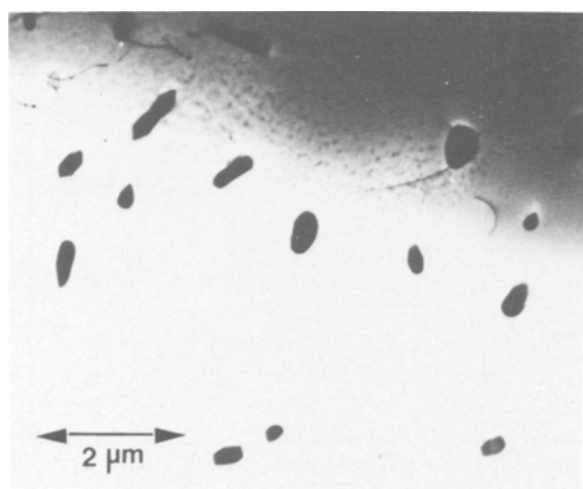


Figure 8 TEM bright field image of deformed specimen showing coarsened precipitates of NiAlNb.

TABLE I Comparison of d -values from powder diffraction (PD) file for NiAlNb with those determined by electron diffraction (ED) from precipitates and X-ray diffraction (XRD) of pulverized homogenized alloy in this study

hkl	PD file	Measured, ED (nm)	Measured, XRD (nm)
100	4.33	0.435	—
002	4.05	0.406	—
101	3.82	0.383	—
102	2.96	0.296	—
201	2.09	0.211	0.210
110	2.50	—	0.247
103	2.29	0.225	0.226
213	1.39	—	0.138
220	1.25	—	0.123

Hexagonal 12H, $a = 0.50$, $c = 0.8093$.

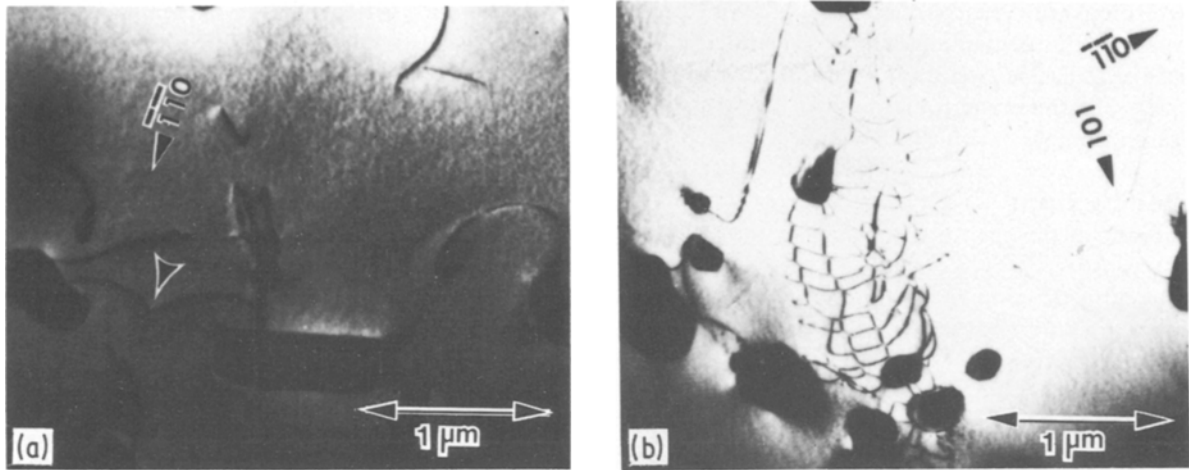


Figure 9 Transmission electron micrographs of deformed specimen illustrating (a) dislocations pinned at and bowing between precipitates and (b) dislocation networks formed between precipitates.

X-ray diffraction of the deformed specimen in a powder form also agreed with the conclusion that the second phase present in the matrix of NiAl is the hexagonal phase NiAlNb. These data are also presented in the same table for comparison. The possi-

bility of the second phase being Ni₂AlNb (a Heusler alloy) was very carefully checked and ruled out.

In terms of the strengthening mechanism in the ternary alloy, since the ternary intermetallic phase NiAlNb is harder than the binary NiAl [6], dislocation motion at the testing temperature appears to be hindered by the presence of these fine precipitates. Such a mechanism is very sensitive to the average spacing between and hence the size of the precipitates for a given volume fraction. Coarsening of these precipitates could, therefore, have dramatic consequences for strengthening. In fact, the drop of flow stress during the test is suspected to have been caused by coarsening of the precipitates from about 50 nm observed in the undeformed, as-homogenized specimen to about 500 nm in the deformed specimen. At the same time, the dislocations present between the precipitates may act as rapid paths for diffusion in the matrix, thereby enhancing the kinetics of the coarsening of the precipitates.

It should be pointed out here that these results are

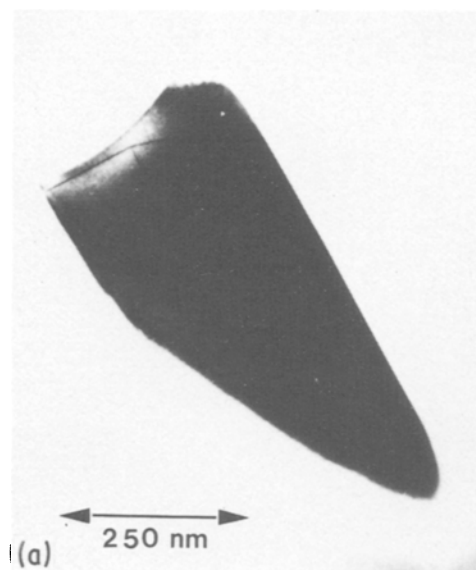
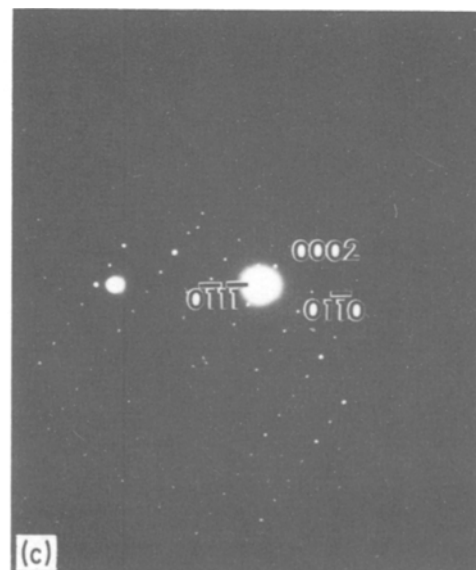
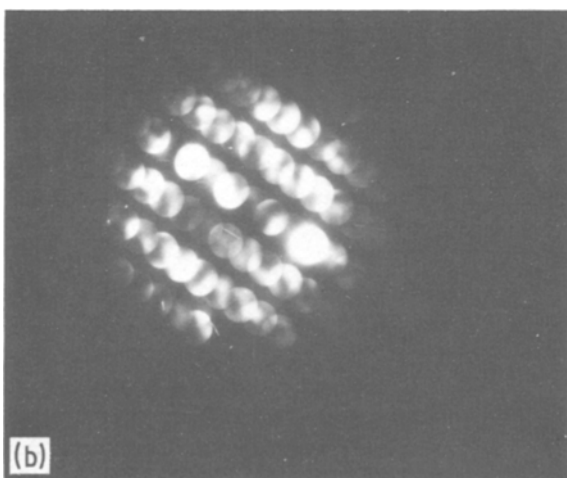


Figure 10 TEM bright field image of a large precipitate in the deformed specimen and corresponding SAD and microdiffraction patterns of a zone axis indexed as (2 $\bar{1}\bar{1}$ 0).



in agreement with the proposed strengthening mechanism in an alloy containing 2 at % Ta [11], investigated in part of the same overall program for investigating the effect of ternary additions on NiAl at NASA Lewis Research Center.

4. Conclusions

The results of this investigation suggest the following conclusions:

1. Homogenization of ternary alloys of NiAl and niobium, prepared by hot extrusion of powder blends of NiAl and niobium, results in the formation of the intermediate phases NiAlNb and NiAlNb₂.

2. The high temperature strengthening of this alloy appears to be due to a dispersion of fine precipitates (~ 50 nm in size) of NiAlNb which have a hexagonal crystal structure. These precipitates interfere with dislocation motion during high temperature deformation.

3. The strengthening precipitates coarsen significantly during the testing (from about 50 to 500 nm) and this coarsening may be responsible for the drop in flow stress during the deformation.

Acknowledgements

The authors would like to acknowledge the support of Sohio Research Center for the use of their microscopy

facilities and NASA Lewis Research Center for supplying the materials.

References

1. "Structural Uses for Ductile Ordered Alloys", NMAB Report 419 (National Academy Press, Washington, DC, 1984).
2. J. R. STEPHENS, in "High Temperature Ordered Intermetallic Alloys", Materials Research Society Symposia Proceedings Vol. 39 (1984) p. 381.
3. N. S. STOLOFF, *Int. Met. Rev.* **29**(3) (1984) 123.
4. C. T. LIU and C. L. WHITE, in "High Temperature Ordered Intermetallic Alloys", Materials Research Society Symposia Proceedings Vol. 39 (1984) p. 365.
5. K. M. VEDULA, V. PATHARE, I. ASLANIDIS and R. H. TITRAN, *ibid.* p. 411.
6. I. I. KORNILOV, R. S. MINTS, L. N. GUSEVA and YU. S. MALKOV, *Russ. Metall.* **6** (1965) 83.
7. J. D. WHITTENBERGER, unpublished results at NASA Lewis Research Center, Cleveland, Ohio.
8. O. D. SHERBY, R. H. KLUNDT and A. K. MILLER, *Met. Trans.* **8A** (1977) 843.
9. G. S. ANSELL and J. WEERTMAN, *Trans. AIME* **215** (1959) 838.
10. J. J. PETROVIC and L. J. EBERT, *Met. Trans.* **4** (1973) 1309.
11. V. M. PATHARE, MS thesis, Case Western Reserve University, Cleveland, Ohio (1984).

Received 24 June

and accepted 9 August 1985